# Joint Precoder and Equalizer Design for Multi-User Multi-Cell MIMO VLC Systems

Helin Yang <sup>10</sup>, Student Member, IEEE, Chen Chen <sup>10</sup>, Wen-De Zhong, Senior Member, IEEE, and Arokiaswami Alphones, Senior Member, IEEE

Abstract-In multi-user multi-cell multiple-input multipleoutput (MIMO) visible light communication (VLC) systems, intercell interference (ICI) and inter-user interference (IUI) are the two key factors that could severely degrade the system performance. In this paper, for the first time, a novel joint precoder and equalizer design based on interference alignment is proposed to mitigate both IUI and ICI in multi-user multi-cell MIMO VLC systems under imperfect channel state information (CSI). The proposed approach aims to choose proper precoder and receiving equalizer to minimize the mean square error (MSE) under the unique optical power constraints in VLC. Furthermore, we consider optical channel estimation error in our formulated joint optimization problem when designing the joint precoder and receiving equalizer in multi-user multi-cell MIMO VLC systems. Numerical results show that the proposed design achieves a better performance under different users locations, channel estimation errors, and transmitter/receiver spacing, compared to the existing minimum mean square error (MMSE) and max-rate designs. Especially, when the transmit optical power is 12 W per light emitting diode (LED) lamp, our proposed design achieves a sum rate improvement of up to 18.2% and 28.7% as compared with the MMSE and maxrate designs, respectively. In addition, the proposed design can save about 1.4 and 4.3 W optical power per LED lamp as compared with the MMSE and max-rate designs, respectively, at a target bit error rate (BER) of  $10^{-3}$ .

Index Terms—Visible light communication, multi-user multicell MIMO, transceiver design, interference alignment, imperfect channel state information.

### I. INTRODUCTION

ISIBLE light communication (VLC) based on white light emitting diodes (LEDs) has been emerging as a promising technology for indoor wireless communications, due to its many distinct advantages such as low cost, abundant bandwidth and free from electromagnetic interference [1]. However, the

Manuscript received May 3, 2018; revised July 13, 2018 and September 10, 2018; accepted October 14, 2018. Date of publication October 18, 2018; date of current version December 14, 2018. This work was supported in part by the National Nature Science Foundation of China under Grant 61502067 and in part by the Key Science and Technology Research Program of Chongqing Municipal Education Commission under Grant KJZD-K201800603. This work was conducted within the Delta-NTU Corporate Lab for Cyber-Physical Systems with funding support from Delta Electronics Inc. and the National Research Foundation Singapore under the CorpLab@University. The review of this paper was coordinated by Dr. K. Adachi. (Corresponding author: Chen Chen.)

The authors are with the School of Electrical and Electronic Engineering, Nanyang Technological University (NTU), Singapore 639798 (e-mail: hyang013@e.ntu.edu.sg; chen0884@e.ntu.edu.sg; ewdzhong@ntu.edu.sg; eal-phones@ntu.edu.sg).

Color versions of one or more of the figures in this paper are available online at http://ieeexplore.ieee.org.

Digital Object Identifier 10.1109/TVT.2018.2876788

capacity of VLC systems is greatly limited by the small modulation bandwidth of LEDs. So far, various techniques have been proposed to enhance the system capacity, such as multiple-input multiple-output (MIMO) transmission [2], [3], frequency domain equalization (FDE) techniques [4], spectral-efficient modulation schemes such as orthogonal frequency division multiplexing (OFDM) [5]–[7], and so on.

Recently, the concept of optical attocells has been introduced in practical VLC systems, where each of the LED lamps creates an optical attocell configuration [8]-[10] and serves multiple users within its illuminated area. Such a cellular indoor VLC system is referred to as a multi-cell VLC system [11], and the respective illumination areas of the adjacent cells are inevitably overlapped with each other. When the users are located in the overlapped area, their performance may be greatly degraded due to the severe inter-cell interference (ICI) [8]-[11]. Various approaches have been proposed to mitigate ICI in multi-cell VLC systems, including color-shift-keying (CSK) modulation [12], digitally filtering signal bands before reception [13], or optical differential detection [14]. However, all the above approaches [10]–[12] require special designs at transmitters or receivers. For example, the CSK modulation should need the use of red, green and blue LEDs, which limits its applications. As an effective way to eliminate ICI, precoding has also been applied in multi-cell VLC systems [11], [15]-[18]. Two linear precoders based on the minimum mean square error (MMSE) method were proposed to minimize the mean-square error (MSE) in multiple coordinated VLC attocells under imperfect channel state information (CSI) [15], [16], where all the LED transmitters are assumed to be coordinated through an optical power line communication (PLC) link. In [17], the authors have studied several forms of cell cooperation in multi-user multi-cell VLC systems, and designed an optimal zero forcing (ZF) precoder to maximize the achievable sum capacity of users. Moreover, two centralized and decentralized transmit power allocation approaches based on optical code division multiple- access technique were developed to support multiple users in multi-cell VLC systems [18], and the MMSE filter at the receiver was designed to diminish ICI effectively.

In indoor MIMO VLC systems, each cell in a multi-cell VLC system is expected to simultaneously support multiple users and each user may receive signals that are broadcasted from the LED transmitters but intended to other users within the same cell. This kind of interference is referred to as the inter-user interference (IUI) [19], which is another critical issue that can

greatly degrade the system performance in multi-user VLC systems. In [19]-[23], the transmitter precoding was proposed to mitigate IUI in multi-user VLC systems. In [20], transmitter precoding design was achieved by solving the sum rate maximization problem subject to the optical power constraints. The work in [21] reported a MIMO OFDM technique in multi- user VLC systems, and investigated the system capacity. In [22], an optical adaptive precoder was proposed to enhance the signal-tointerference-plus-noise ratio (SINR) performance in multi-user MIMO VLC systems. However, the precoders in [19]–[23] were only proposed for single-cell VLC systems where only the IUI was considered while the ICI was neglected. In practical applications, both ICI and IUI should be taken into consideration when implementing an indoor multi-user multi- cell MIMO VLC system. In recent years, the interference alignment (IA) technique has been proposed to efficiently separate the desired signal from the interference in wireless radio frequency (RF) communication systems [24]–[27], which has also been applied in VLC systems. In [28], [29], IA was explored in a multi-user VLC system by assuming perfect CSI. However, the CSI is not always perfectly available at LED transmitters [30], [31], and the assumption of perfect CSI is not practical for VLC systems. Hence, a blind IA scheme was proposed to achieve the system capacity without CSI at the transmitter in multi-user MIMO VLC systems [32]. However, the works in [23], [32] only considered a single cell, and did not extend the framework to multi-cell VLC systems where the ICI mitigation is a key challenge. As a result, how to design the precoder or equalizer to mitigate both ICI and IUI for indoor multi-user multi-cell MIMO VLC systems is still a key challenge.

In this paper, we firstly propose a novel joint precoder and equalizer design based on IA to mitigate both ICI and IUI for multi-user multi-cell MIMO VLC systems in the presence of imperfect CSI. To achieve the optimal transmit precoder and receiving equalizer, we formulate the joint optimization problem through minimizing the mean-squared error (MSE) under the unique optical power constraints (real-valued and non-negative transmitted signals and the output optical power of each LED transmitter should be controlled in the limited linear range [16], [19], [30]) in VLC, which is different from the transceiver design in RF communication systems [33], [34]. The proposed design aims to mitigate both the IUI and ICI effectively, as well as maintain the bit error rate (BER) at the lowest level. Furthermore, we take into account the channel estimation error in our formulated joint optimization problem when designing the optimal precoder and receiving equalizer in multi-user multi-cell MIMO-VLC systems. We investigate the impact of different users locations, channel estimation errors and LED/photodetector (PD) spacing levels on the system capacity and BER performance. Numerical results show that the proposed design achieves higher system capacity and BER improvements under imperfect CSI, compared with the existing MMSE and max-rate designs.

The rest of this paper is organized as follows. In Section II, we describe the model of a multi-user multi-cell MIMO-VLC system. Section III presents the joint precoder and equalizer design based on IA, and the solution to the optimization problem is also

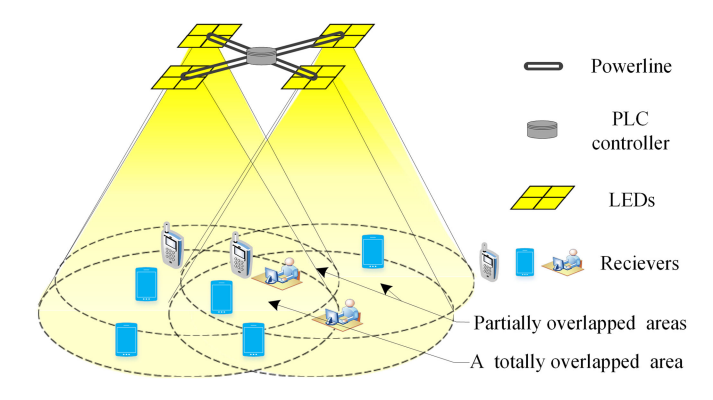


Fig. 1. An indoor four-cell MIMO VLC system with the overlapped areas.

provided. The analysis in terms of the behavior of the proposed design is presented in Section IV. Section V provides the simulation results and discussions. Finally, Section VI concludes the paper.

Notation:  $\mathbf{I}_N$  denotes an identity matrix.  $E[\cdot]$  is the expectation operator.  $R^{N\times M}$  denotes the set of  $N\times M$  dimensional real-valued numbers,  $R_+^{N\times M}$  represents the set of  $N\times M$  dimensional non-negative real-valued numbers.  $(\cdot)^T$ ,  $\mathrm{Tr}\{\cdot\}$  and  $(\cdot)^{-1}$  denote the transpose, the trace and the inverse of a matrix/vector, respectively.  $||\cdot||_F$  denotes the Frobenius norm,  $||\cdot||_l$  denotes the l-norm,  $\mathrm{vec}(\cdot)$  is the vectorization operator, and  $\otimes$  denotes the Kronecker product.  $\mathrm{abs}(\cdot)$  denotes an elementwise absolute operator and 1 denotes a vector whose elements are all 1.

## II. SYSTEM MODEL

In practical indoor environments, multiple LED lamps are usually installed to set up a VLC system to satisfy lighting and communication requirements of users, as shown in Fig. 1. As in [16], we assume that these LED lamps fully cooperate with each other through a PLC backbone network to broadcast information to multiple users simultaneously, and exchange the users information (such as the channel gains) with each LED lamp through the PLC controller in the VLC system. There are multiple LED lamps establishing optical attocells to communicate with multiple users within its illuminated area, where each cell has multiple LED lamps and each user is equipped with multiple PDs [8]–[10]. Such a cellular indoor VLC system is referred to as a multi-user multi-cell MIMO VLC system in this paper.

#### A. Transmitter Model

In the multi-user multi-cell MIMO-VLC system, some users suffer from ICI when they are located in the overlapped areas in addition to the IUI. Especially, the users who are located in the completely overlapped area may suffer from severe ICI, leading to the drastic performance degradation. We assume that the VLC system has B cells and broadcasts information to K users with each user being equipped with Nr PDs. Each cell has Nt down-facing LEDs as transmitters. The k-th user in cell b is

denoted as the user . In this paper, we consider the on-off keying (OOK) modulation as it is typically applied in VLC systems, and  $s_{k,b} \in$  define as the data stream transmitted to the user (k,b).  $s_{k,b}$  is assumed to be a non-return-to-zero (NRZ) OOK signal which has a zero mean (i.e.,  $E\{s_{k,b}\}=0$ ) . Since VLC systems employ the intensity modulation/direct detection (IM/DD) technique, the transmitted signal should be real-valued and non-negative. This means that a direct current (DC) component should be added to make sure the transmitted data is non-negative. In addition, LEDs have a limited linear drive current range where the output optical power linearly increases with the drive current [35].

With the transmitter precoding strategy and the DC component addition, the signal vector transmitted by the LED lamps in cell b can be expressed as

$$\mathbf{x}_b = \mathbf{V}_b \mathbf{s}_b + \mathbf{p}_b = \sum_{k=1}^K \mathbf{v}_{k,b} s_{k,b} + \mathbf{p}_b$$
 (1)

where  $\mathbf{V}_b = [\mathbf{v}_{1,b}, \dots, \mathbf{v}_{k,b}, \dots, \mathbf{v}_{K,b}]$  is the precoding matrix in cell b and  $\mathbf{v}_{k,b} \in R^{N_t} \times 1$  is the precoding vector for the user (k,b);  $\mathbf{s}_b = [s_{1,b}, \dots, s_{k,b}, \dots, s_{K,b}]^{\mathrm{T}}$  is the real-valued source symbol vector; and  $\mathbf{p}_b = [p_{1,b}, \dots, p_{N_t,b}]^{\mathrm{T}} \in R_+^{N_t \times 1}$  denotes the DC offset optical power vector which is used to guarantee the non-negativity of the transmitted signal and adjust the illumination level in the room. The signal  $x_{n,b}$  transmitted by the n-th LED lamp in cell b can be given by

$$x_{n,b} = \sum_{k=1}^{K} v_{n,k,b} s_{k,b} + p_{n,b}$$
 (2)

where  $v_{n,k,b}$  is the element of  $\mathbf{V}_b$  in the n-th row and k-th column. From (1) and (2), the non-negative transmitted signal in VLC systems imposes the optical constraints on the precoding matrix  $\mathbf{V}_b$  in each cell. Since we choose the OOK modulation with  $s_{k,b} \in \{\pm 1\}$ , the data signal before adding the DC offset at the n-th LED lamp in cell b satisfies

$$-\sum_{k=1}^{K} |v_{n,k,b}| \le \sum_{k=1}^{K} v_{n,k,b} s_{k,b} \le \sum_{k=1}^{K} |v_{n,k,b}|$$
 (3)

In order to ensure that LED lamps can operate in the limited liner optical power range, the data signal transmitted at each LED lamp satisfies

$$-\sum_{k=1}^{K} |v_{n,k,b}| + p_{n,b} \le x_{n,b} \le \sum_{k=1}^{K} |v_{n,k,b}| + p_{n,b}$$
 (4)

To ensure that the LED lamp drive optical power in the linear region of  $[p_{\min}, p_{\max}]$ , where  $p_{\min}$  and  $p_{\max}$  denote the minimum and maximum values of the optical power. Then, combining (2), (3) and (4), we have

$$\begin{cases} p_{n,b} - \sum_{k=1}^{K} |v_{n,k,b}| \ge p_{\min} \\ p_{n,b} + \sum_{k=1}^{K} |v_{n,k,b}| \le p_{\max} \end{cases}$$
 (5)

Rearranging the inequalities in (5), we can get the constraint of each precoding element of  $V_b$ 

$$\sum_{k=1}^{K} |v_{n,k,b}| = \|\mathbf{v}_{n,b}\|_{1}$$

$$\leq \min \{p_{n,b} - p_{\min}, \ p_{\max} - p_{n,b}\}, \ \forall n, \ \forall b \ \ (6)$$

where  $\mathbf{v}_{n,b}$  is the *n*-th row vector of  $\mathbf{V}_b$ . The constraint in (6) enables to select available precoding matrix  $\mathbf{V}_b$  in practical indoor environments.

## B. Receiver Model

At the receiver, the received signal is detected by the PDs of each user and converted back to a digital signal. Then, for the user (k,b), the received signal after the direct detection can be given by

$$\mathbf{y}_{k,b} = \underbrace{\mathbf{H}_{k,b}^{b} \mathbf{v}_{k,b} s_{k,b}}_{\text{desired signal}} + \underbrace{\sum_{b' \neq b}^{B} \rho_{k,b}^{b'} \sum_{m=1}^{K} \mathbf{H}_{k,b}^{b'} \mathbf{v}_{m,b'} s_{m,b'}}_{\text{ICI}} + \underbrace{\sum_{\ell=1,\ell \neq k}^{K} \mathbf{H}_{k,b}^{b} \mathbf{v}_{\ell,b} s_{\ell,b}}_{\text{IUI}} + \underbrace{\left(\mathbf{H}_{k,b}^{b} \mathbf{p}_{b} + \sum_{b' \neq b}^{B} \rho_{k,b}^{b'} \mathbf{H}_{k,b}^{b'} \mathbf{p}_{b'}\right)}_{\text{DCbias}}$$

$$+ \mathbf{n}_{k,b}$$

$$(7)$$

where  $\rho_{k,b}^{b'}$  denotes a set of binary variables, i.e.,  $\rho_{k,b}^{b'} \in \{0,1\}$ , which indicates whether the user (k,b) receives ICI from the adjacent cell b' or not. If the user (k,b) receives ICI from the cell b', then  $\rho_{k,b}^{b'} = 1$ ; otherwise  $\rho_{k,b}^{b'} = 0$ .  $\mathbf{H}_{k,b}^{b'} \in R_+^{N_r \times N_t}$  denotes the optical channel matrix from the LED lamps in cell b' to the user (k,b). In (7), we can see that the received signal consists of five terms. The first term is the desired signal, the second and third terms are the ICI and IUI, respectively, the fourth term is the DC offset, and the last one is the additive Gaussian noise vector with zero-mean and variance of  $\delta_{k,b}^2$ , which consists of the shot noise and thermal noise in VLC systems [15]. We define  $h_{k,b,b'}^{j,i}$  as the optical channel gain from the j-th LED lamp in cell b' to the i-th PD of the user (k,b), and  $h_{k,b,b'}^{j,i}$  is one of the elements of  $\mathbf{H}_{k,b}^{b'}$ .  $\psi_{k,b,b'}^{j,i}$  and  $\psi_c$  denote the angle of incidence and the halfangle field-of-view (FOV) of the receiver, respectively. When  $0 \leq \psi_{k,b,b'}^{j,i} \leq \psi$ ,  $h_{k,b,b'}^{j,i}$  can be expressed as

$$h_{k,b,b'}^{j,i} = \frac{A_{k,b,b'}^{j,i}}{(d_{k,b,b'}^{j,i})^2} R_0(\phi_{k,b,b'}^{j,i}) T_s(\psi_{k,b,b'}^{j,i}) g(\psi_{k,b,b'}^{j,i}) \cos \psi_{k,b,b'}^{j,i}$$
(8)

where  $A_{k,b,b'}^{j,i}$  is the active area of the PD,  $\phi_{k,b,b'}^{j,i}$  is the angle of irradiance,  $d_{k,b,b'}^{j,i}$  denotes the distance and  $T_s(\psi_{k,b,b'}^{j,i})$  is optical filter gain.  $g(\psi_{k,b,b'}^{j,i})$  is the optical concentrator gain. If  $0 \le \psi_{k,b,b'}^{j,i} \le \psi_c$ ,  $g(\psi_{k,b,b'}^{j,i}) = \eta/\sin^2\!\psi_c$ ; otherwise,  $g(\psi_{k,b,b'}^{j,i}) = 0$ , where  $\eta$  is the refractive index. Assuming that the LEDs radiation pattern is modelled as the Lambertian pattern, the

radiant intensity  $R_0(\phi_{k,b,b'}^{j,i})$  can be expressed as:  $R_0(\phi_{k,b,b'}^{j,i}) = (\vartheta+1)\cos^{\vartheta}(\phi_{k,b,b'}^{j,i})/2\pi$ , where  $\vartheta=\ln 2/(\ln\cos\phi_{1/2})$  denotes the order of Lambertian emission with  $\phi_{1/2}$  being the LEDs semi-angle at half power.

Applying the linear equalizers at receivers, the user (k,b) achieves its own desired signal by equalizing the received signal through multiplying a receiving equalizer vector  $\mathbf{u}_{k,b} \in R^{N_r \times 1}$ . Then, the signal for the user (k,b) after DC removal can be expressed as

$$\tilde{\mathbf{y}}_{k,b} = \sum_{b'=1}^{B} \sum_{m=1}^{K} \rho_{k,b}^{b'} \mathbf{u}_{k,b}^{\mathrm{T}} \mathbf{H}_{k,b}^{b'} \mathbf{v}_{m,b'} s_{m,b'} + \mathbf{u}_{k,b}^{\mathrm{T}} \mathbf{n}_{k,b}$$
(9)

From (9), the system aims to properly mitigate the interference (IUI and ICI) and recover the desired signal for each user successfully. As multiple LED lamps are cooperating with each other based on a PLC controller, different cells can exchange information (channel state information, precoders and DC offset) to perform the proposed design based on IA, which will be discussed in the next section.

## III. IA BASED JOINT PRECODER AND EQUALIZER DESIGN

In this section, we propose a novel joint precoder and receiving equalizer design based on IA for multi-user multi-cell MIMO VLC systems. As each user aims to recover its own desired signal successfully, the interference (IUI and ICI) should be aligned into the subspace that is orthogonal to the receiving equalizer  $\mathbf{u}_{k,b}$ , and the dimension of the signal space of the desired signal needs to be equal to the number of the data streams. Therefore, the conditions for the ideal IA under perfect CSI are given as follows [24]–[27]

$$\mathbf{u}_{k,b}^{\mathrm{T}} \mathbf{H}_{k,b}^{b} \mathbf{v}_{\ell,b} = 0, \quad \forall \ell \neq k$$
 (10a)

$$\mathbf{u}_{k,h}^{\mathrm{T}} \mathbf{H}_{k,h}^{b'} \mathbf{v}_{m,b'} = 0, \quad \forall b' \neq b, \forall m \tag{10b}$$

$$\operatorname{rank}\left\{\mathbf{u}_{k,b}^{\mathrm{T}}\mathbf{H}_{k,b}^{b}\mathbf{v}_{k,b}\right\} = d, \quad \forall k, b$$
 (10c)

$$\mathbf{v}_{k,b}^{\mathrm{T}}\mathbf{v}_{k,b} = I_d, \mathbf{u}_{k,b}^{\mathrm{T}}\mathbf{u}_{k,b} = \mathbf{I}_d$$
 (10d)

where d is the number of transmitted data streams, and we set d=1 in this paper. In addition, (10a) and (10b) imply that both IUI and ICI are perfectly mitigated, and (10c) satisfies the number of the transmitted data streams per user. The goal of the IA scheme in multi-user multi-cell MIMO VLC systems is to design optimal precoders and receiving equalizers as in (10a)–(10c) to align the unwanted IUI and ICI without suppressing the desired signal at each receiver. In addition, the subjection in (10d) shows the precoder  $\mathbf{v}_{k,b}$  and receiving equalizer  $\mathbf{u}_{k,b}$  being orthogonal, which has the same goal with the conditions in (10a), (10b) and (10c) when we apply the IA scheme [24]–[27].

However, the standard IA schemes are sensitive to the channel estimation error [24]–[27], [36]. Under the practical channel conditions, both IUI and ICI cannot be perfectly mitigated, resulting in the performance degradation in VLC systems. Therefore, in the following subsection, we will consider the channel estimation error in our proposed design.

## A. Channel Uncertainty Model

In practical MIMO VLC systems, the CSI is not perfectly available, and hence the channel estimation error should be taken into account. We set  $\mathbf{H}_{k,b}^{b'}$  and  $\hat{\mathbf{H}}_{k,b}^{b}$  as the perfect CSI and estimated CSI, respectively, and  $\Delta \hat{\mathbf{H}}_{k,b}^{b'}$  is the channel estimation uncertainty which is assumed as the Gaussian model with zero mean and covariance matrix  $\{\Delta \hat{\mathbf{H}}_{k,b}^{b'}\Delta \hat{\mathbf{H}}_{k,b}^{b'}\} = \delta_e^2 \mathbf{I}_d$  [16]. We assume that  $\Delta \hat{\mathbf{H}}_{k,b}^{b'}$  is independent of  $\hat{\mathbf{H}}_{k,b}^{b'}$  [16]. For simplicity, we assume all channel uncertainties  $\{\Delta \hat{\mathbf{H}}_{k,b}^{b'}\}$  have an equal variance  $\delta_e^2$ .

Then, considering the estimation inaccuracy, the channel matrix  $\hat{\mathbf{H}}_{k,b}^{b'}$  and the norm-bounded channel uncertainty  $\Delta \hat{\mathbf{H}}_{k,b}^{b'}$  can be given by [16]

$$\mathbf{H}_{k,b}^{b'} = \hat{\mathbf{H}}_{k,b}^{b} + \Delta \hat{\mathbf{H}}_{k,b}^{b}$$

$$\Omega_{k,b}^{b'} = \left\{ \Delta \hat{\mathbf{H}}_{k,b}^{b'} \middle| \operatorname{Tr} \left\{ \Delta \hat{\mathbf{H}}_{k,b}^{b'} \Delta \hat{\mathbf{H}}_{k,b}^{b'T} \right\} \le \varepsilon \right\}$$
(11)

where  $\varepsilon$  is the radius of the channel uncertainty region. For simplicity, we assume that the channel uncertainty regions of all channel gains are the same.

#### B. MMSE

In order to recover the data from the received signal, we design the optimal precoder and receiving equalizer based on the MMSE criterion, i.e., minimizing the MSE of each user in the VLC system. Then, the MSE between the recovered data and the transmitted data of the user (k,b) can be expressed as

$$\Phi_{\text{MSE},k,b} = \left[ \left\| \mathbf{u}_{k,b}^{\text{T}} \mathbf{y}_{k,b} - s_{k,b} \right\|_{F}^{2} \right] \\
= \left[ \text{Tr} \left\{ \left( \mathbf{u}_{k,b}^{\text{T}} \mathbf{y}_{k,b} - s_{k,b} \right) \left( \mathbf{u}_{k,b}^{\text{T}} \mathbf{y}_{k,b} - s_{k,b} \right)^{\text{T}} \right\} \right] \\
= \left[ \mu^{2} \text{Tr} \left\{ \sum_{b'=1}^{B} \sum_{m=1}^{K} \mathbf{u}_{k,b}^{\text{T}} \mathbf{H}_{k,b}^{b'} \mathbf{v}_{m,b'} \mathbf{v}_{m,b'}^{\text{T}} \mathbf{H}_{k,b}^{b'} \mathbf{u}_{k,b} - \mathbf{v}_{k,b}^{\text{T}} \mathbf{H}_{k,b}^{b'} \mathbf{u}_{k,b} - \mathbf{u}_{k,b}^{\text{T}} \mathbf{H}_{k,b}^{b'} \mathbf{v}_{k,b} \right] \right\} + \mu^{2} \quad (12)$$

In (12), we assume the transmitted data  $\{s_{k,b}s_{m,b'}\}=0$ ,  $k \neq \ell$  and  $b' \neq b$ , and the noise vector  $\mathbf{n}_{k,b}$  are independent of  $s_{k,b}$  and  $\mathbf{H}^b_{k,b}$  [26], [30]. denotes the covariance of  $\mu^2$ .

The objective function  $\Phi_{\mathrm{MSE},k,b}$  in (12) doesn't consider the channel estimation error. Taking the channel uncertainty (11) into account, the function in (12) can be modified as

$$\widehat{\mathbf{\Phi}}_{\mathrm{MSE},k,b} \leq \mu^{2} \mathrm{Tr} \left( \mathbf{u}_{k,b}^{\mathrm{T}} \left[ \sum_{b'=1}^{B} \sum_{m=1}^{K} \widehat{\mathbf{H}}_{k,b}^{b'} \mathbf{v}_{m,b'} \mathbf{v}_{m,b'}^{\mathrm{T}} \widehat{\mathbf{H}}_{k,b}^{b'\mathrm{T}} \right] + \sum_{b'=1}^{B} \sum_{m=1}^{K} \varepsilon \mathrm{Tr} \left\{ \mathbf{v}_{m,b'} \mathbf{v}_{m,b'}^{\mathrm{T}} \right\} \mathbf{I}_{N_{r}} \mathbf{u}_{k,b} - \mathbf{v}_{k,b}^{\mathrm{T}} \widehat{\mathbf{H}}_{k,b}^{b'\mathrm{T}} \mathbf{v}_{k,b} + \mu^{2} \quad (13)$$

From (12) and (13), our goal is to design the optimal transmit precoder  $\mathbf{v}_{k,b}$  and receiving equalizer  $\mathbf{u}_{k,b}$  based on IA to minimize the MSE for the multi-user multi-cell VLC system while satisfying the optical power constraints (6). Then, the optimization problem can be formulated as

$$\min_{\mathbf{v}_{k,b},\mathbf{u}_{k,b},\forall k,\forall b} \sum_{b=1}^{B} \sum_{k=1}^{K} \widehat{\Phi}_{\mathrm{MSE},k,b}$$
 (14a)

s.t. 
$$\mathbf{v}_{k,b}^{\mathrm{T}} \mathbf{v}_{k,b} = I_d, \forall k, \forall b$$
 (14b)

$$\mathbf{u}_{k,b}^{\mathrm{T}}\mathbf{u}_{k,b} = \mathbf{I}_d, \forall k, \forall b \tag{14c}$$

$$\|\mathbf{v}_{n,b}\|_{1} \le \min\{p_{n,b} - p_{\min}, p_{\max} - p_{n,b}\}, \forall n, \forall b$$
 (14d)

## C. Solution for Joint Precoder and Equalizer Design

As we can see, the problem in (14) is a joint optimization problem since the transmit precoders and receiving equalizers are involved and the optimization problem in (14) is not convex with these variables, which is hard to solve in general. Here, we divide it into two subproblems and solve them individually, and then optimize the precoder and equalizer iteratively by applying an iteration scheme.

1) Transmit Precoder Selection: Without loss of generality, we aim to achieve the optimal precoder of each cell by solving the problem in (14) when the receiving equalizer set  $\{\mathbf{u}_{k,b}\}$  of all users in all cells are given. However, it is hard to implement the traditional optimization algorithms with the relaxations due to the element-wise absolute operator in the constraint (14d). Hence, we apply a matrix analysis to transform the optimization problem into a convex linearly constrained quadratic program (LCOP) [37]. According to the matrix analysis [37], we have the properties that  $Tr{ABA^T} = vec(A)(B \otimes I)vec(A)^T$  and  $Tr{AB} = Tr{BA}$ . In the VLC system, the matrixes and vectors are all real values, hence the first part of the objective function in (13) is rewritten as

$$\operatorname{Tr}\left\{\mathbf{u}_{k,b}^{\mathrm{T}}\hat{\mathbf{H}}_{k,b}^{b'}\mathbf{v}_{\mathrm{m},b'}\mathbf{v}_{\mathrm{m},b'}^{\mathrm{T}}\hat{\mathbf{H}}_{k,b}^{b'\mathrm{T}}\mathbf{u}_{k,b}\right\}$$

$$= vec(\mathbf{v}_{m,b'}^{\mathrm{T}})^{\mathrm{T}}\left(\hat{\mathbf{H}}_{k,b}^{b'\mathrm{T}}\mathbf{u}_{k,b}\mathbf{u}_{k,b}^{\mathrm{T}}\hat{\mathbf{H}}_{k,b}^{b'}\otimes\mathbf{I}_{N_{r}}\right)vec(\mathbf{v}_{m,b'}^{\mathrm{T}})$$
(15)

The above term is quadratic and hence other parts in (13) are linear or constant. For the above analysis, we can transform the optimization problem in (14) into a convex LCQP problem. And a Matlab software package is used to solve convex LCQP problems based on the semi-definite programming (SDP) (called CVX [38]), which can effectively achieve the optimal precoder  $V_b$  of each cell by solving the transformed problem when the receiving equalizer set  $\{\mathbf{u}_{k,b}\}$  of all users in all cells are given.

2) Receiving Equalizer Selection: Since the constraint (14d) has nothing to do with the equalizer at each receiver, when the precoder  $V_b$  of each cell is given, the corresponding optimization problem under the channel estimation error can be **Algorithm 1:** Iterative Scheme for the Joint Design of  $\mathbf{v}_{k,b}$ and  $\mathbf{u}_{k,b}$ .

### **Initialization:**

- 1: Set the optical power level  $\mathbf{p}_b$  for each cell;
- 2: Initialize the unitary precoder matrix  $\mathbf{v}_{k,b}$ ,  $\forall k, \forall b$  and satisfy the constraint (14d)
- 3: Set the desired accuracy  $\zeta$  and the maximum number of iterations  $N^{\max}$ , let n=1;

## Repeat:

- 4: Given the precoder set  $\{V_b\}_{b=1}^B$ , compute  $\mathbf{u}_{k,b}$  based on
- 5: With all the receiving equalizer  $\mathbf{u}_{k,b}$ ,  $\forall k$ ,  $\forall b$ , update  $\mathbf{v}_{k,b}$ by using the CVX software;
- 6: n:=n+1; 7: Until  $\frac{1}{B}\sum_{b=1}^{B}||\mathbf{V}_b(n)-\mathbf{V}_b(n)||^2 \leq \zeta$  or  $n\geq N^{\max}$ , go to the next step;

**Output:**  $\mathbf{v}_{k,b}$  and  $\mathbf{u}_{k,b}$ ,  $\forall k$ ,  $\forall b$ .

expressed as

$$\min_{\mathbf{u}_{k,b},\forall k,\forall b} \sum_{b=1}^{B} \sum_{k=1}^{K} \widehat{\Phi}_{\mathrm{MSE},k,b}$$
 (16a)

s.t. 
$$\mathbf{u}_{k,b}^{\mathrm{T}} \mathbf{u}_{k,b} = \mathbf{I}_d, \forall k, \forall b$$
 (16b)

In order to achieve the receiving equalizer  $\mathbf{u}_{k,b}$ , we differentiate  $\Phi_{\text{MSE},k,b}$  with respect to  $\mathbf{u}_{k,b}$  [22], and get the following equation

$$\frac{\partial \widehat{\mathbf{\Phi}}_{\mathrm{MSE},k,b}}{\partial \mathbf{u}_{k,b}} = \mathbf{u}_{k,b}^{\mathrm{T}} \left( \sum_{b'=1}^{B} \sum_{m=1}^{K} \widehat{\mathbf{H}}_{k,b}^{b'} \mathbf{v}_{m,b'} \mathbf{v}_{m,b'}^{\mathrm{T}} \widehat{\mathbf{H}}_{k,b}^{b'\mathrm{T}} + \sum_{b'=1}^{B} \sum_{m=1}^{K} \varepsilon \mathrm{Tr} \left\{ \mathbf{V}_{m,b'} \mathbf{V}_{m,b'}^{\mathrm{T}} \right\} \mathbf{I}_{N_{r}} \right) - \mathbf{V}_{k,b}^{T} \widehat{\mathbf{H}}_{k,b}^{b'\mathrm{T}} \tag{17}$$

Then, we set  $\partial \Phi_{\mathrm{MSE},k,b}/\partial \mathbf{u}_{k,b}$  equal to zero, the optimal receiving equalizer for the user (k, b) can be obtained by

$$\mathbf{u}_{k,b}^{*} = \left(\sum_{b'=1}^{B} \sum_{m=1}^{K} \hat{\mathbf{H}}_{k,b}^{b'} \mathbf{v}_{m,b'} \mathbf{v}_{m,b'}^{\mathrm{T}} \hat{\mathbf{H}}_{k,b}^{b'\mathrm{T}} + \sum_{b'=1}^{B} \sum_{m=1}^{K} \varepsilon \operatorname{Tr} \left\{ \mathbf{v}_{m,b'} \mathbf{v}_{m,b'}^{\mathrm{T}} \right\} \mathbf{I}_{N_{r}} \right)^{-1}$$
(18)

3) Iterative Algorithm: We apply an iterative method to update the precoder  $\mathbf{v}_{k,b}$  and receiving equalizer  $\mathbf{u}_{k,b}$  for all users in all cells iteratively, which is concisely presented in Algorithm 1. The objective function in (14a) are reduced iteratively through adjusting and updating  $\mathbf{v}_{k,b}$  and  $\mathbf{u}_{k,b}$  at each iteration. Hence, we can achieve the optimal precoder and receiving equalizer iteratively, and terminates when it converges. After solving the optimization of the transmit precoder and receiving equalizer in the PLC controller, the LED transmitters will send the information of the equalizer to each user [16], [19], [13], [30]. In addition, we will give the convergence analysis in the next section.

## IV. PERFORMANCE ANALYSIS

#### A. Data Rate Loss

In this subsection, we analyze the data rate loss performance of the proposed design. The data rate of the user (k, b) under the channel estimation error is given by  $R_{k,b} = \log_2(1 + \gamma_{k,b})$ , and  $\gamma_{k,b}$  is the received SINR, which can be given by

$$\gamma_{k,b} = \frac{\left\| \mathbf{u}_{k,b}^{\mathrm{T}} (\hat{\mathbf{H}}_{k,b}^b + \Delta \hat{\mathbf{H}}_{k,b}^b) \mathbf{v}_{k,b} \right\|^2}{I_{k,b} + \delta_{k,b}^2}$$
(19)

where  $I_{k,b}$  is the total interference of IUI and ICI to the user  $I_{k,b} = \sum_{\ell \neq k}^K \|\mathbf{u}_{k,b}^{\mathrm{T}}(\hat{\mathbf{H}}_{k,b}^b + \Delta \hat{\mathbf{H}}_{k,b}^b)\mathbf{v}_{\ell,b}\|^2 + \sum_{b' \neq b}^B \rho_{k,b}^{b'} \sum_{m=1}^K ||\mathbf{u}_{k,b}^{\mathrm{T}}(\hat{\mathbf{H}}_{k,b}^{b'} + \Delta \hat{\mathbf{H}}_{k,b}^{b'})\mathbf{v}_{m,b'}||^2.$ 

Firstly, we define the rate loss of the user as (k,b) as  $\Delta R_{k,b}$ , which is the difference between the ideal data rate  $\tilde{R}_{k,b}$  of the user (k,b) with the ideal joint precoder and equalizer design (where full CSI is known in advance) and the data rate  $R_{k,b}$  with our proposed design. Then, the rate loss of the user (k,b) is expressed as

$$\Delta R_{k,b} = \tilde{R}_{k,b} - R_{k,b}$$

$$= E \left[ \log_2 \left( \delta_{k,b}^2 + \left\| \tilde{\mathbf{u}}_{k,b}^{\mathrm{T}} \mathbf{H}_{k,b}^b \tilde{\mathbf{v}}_{k,b} \right\|^2 \right) \right]$$

$$- E \left[ \log_2 \left( \delta_{k,b}^2 + I_{k,b} + \left\| \mathbf{u}_{k,b}^{\mathrm{T}} \mathbf{H}_{k,b}^b \mathbf{v}_{k,b} \right\|^2 \right) \right]$$

$$- E_{\Delta} \left[ \log_2 \left( \delta_{k,b}^2 \right) \right] + E \left[ \log_2 \left( I_{k,b} + \delta_{k,b}^2 \right) \right]$$
(20)

where  $\tilde{\mathbf{v}}_{k,b}$  and  $\tilde{\mathbf{u}}_{k,b}$  denote the ideal precoder and receiving equalizer for the user (k,b). Since  $I_{k,b} \geq 0$ , and  $\log(\cdot)$  is a strictly monotonically increasing function, we can obtain

$$\Delta R_{k,b} \leq E \left[ \log_2 \left( \delta_{k,b}^2 + \left\| \tilde{\mathbf{u}}_{k,b}^{\mathrm{T}} \mathbf{H}_{k,b}^b \tilde{\mathbf{v}}_{k,b} \right\|^2 \right) \right]$$

$$- E \left[ \log_2 \left( \delta_{k,b}^2 + \left\| \mathbf{u}_{k,b}^{\mathrm{T}} \mathbf{H}_{k,b}^b \mathbf{v}_{k,b} \right\|^2 \right) \right]$$

$$+ E \left[ \log_2 \left( 1 + \frac{I_{k,b}}{\delta_{k,b}^2} \right) \right]$$
(21)

Note  $E[\log_2(1+||\tilde{\mathbf{u}}_{k,b}^{\mathrm{T}}\mathbf{H}_{k,b}^b\tilde{\mathbf{v}}_{k,b}||^2)] = E[\log_2(1+||\mathbf{u}_{k,b}^{\mathrm{T}}\mathbf{H}_{k,b}^b\mathbf{v}_{k,b}||^2)]$ , based on the Theorem 1 in [39]. Using the Jensens inequality, the upper bound of the data rate loss of the user is

$$\Delta R_{k,b} \le E \left[ \log_2 \left( 1 + I_{k,b} / \delta^2 \right) \right] \le \log_2 \left( 1 + E \left[ I_{k,b} \right] / \delta_{k,b}^2 \right)$$
(22)

From (20)–(22), we can comprehend that one of the key effects on the data rate loss is determined by the power of the interference leakage, such as IUI and ICI. Therefore, the design of the precoder  $\mathbf{v}_{k,b}$  and receiving equalizer  $\mathbf{u}_{k,b}$  is important in the multi-user multi-cell MIMO VLC systems. Hence, this paper proposes the joint precoder and equalizer design based on IA for ICI and IUI mitigation in multi-user multi-cell MIMO VLC systems.

## B. Convergence of the Proposed Design

For the optimization problem in (14), we can observe that the proposed design based on IA aims to minimize the objective function in (14a) by using the iterative method to update the precoder  $\mathbf{v}_{k,b}$  and receiving equalizer  $\mathbf{u}_{k,b}$ ,  $k = 1, \dots, K, b =$  $1, \ldots, B$ . Firstly, we minimize the objective function (14a) by fixing the set of the variables  $\mathbf{u}_{k,b}$ ,  $k = \dots, K$ ,  $b = \dots, B$ , so that the optimization problem in (14) reduces to a convex function of the variables  $\mathbf{v}_{k,b}$ ,  $k = 1, \dots, K$ ,  $b = 1, \dots, B$ , which can be solved by using the CVX tool. Then, by giving a set of the precoder variables  $\mathbf{v}_{k,b}$ ,  $k=1,\ldots,K$ ,  $b=1,\ldots,B$ , we obtain the receiving equalizer variables  $\mathbf{u}_{k,b}, k = 1, \dots, K$ ,  $b = \dots, B$  by minimizing the objective function (14a). The objective function is nonnegative, and it is reduced by adjusting the set of precoder and receiving equalizer variables at each iteration. As a result, the convergence of the proposed design can be achieved [26].

# C. Comparison With Existing Popular Designs

Generally, the MMSE design [15], [16], [30] and the sum-rate maximization design [20] are the two existing popular designs applied to improve the system performance in VLC systems. However, the works in [15], [16], [30] only investigated the system performance in single-cell VLC systems without considering ICI mitigation or in multi-cell VLC systems without considering IUI mitigation. Hence, when applying these two designs in multi-user multi-cell MIMO VLC system, the optimization problems can be expressed as follows:

i) The joint precoder and receiving equalizer design based on MMSE [15], [16], [19], [30] (denoted as the MMSE design):

$$\min_{\mathbf{V}_{k,b}, \mathbf{U}_{k,b}, \forall k, \forall b} \left[ ||\mathbf{u}_{k,b}^{\mathrm{T}} \mathbf{y}_{k,b} - s_{k,b}||_F^2 \right]$$
 s.t.  $\|\mathbf{v}_{n,b}\|_1 \leq \min \left\{ p_{n,b} - p_{\min}, \ p_{\max} - p_{n,b} \right\}, \ \forall n, \ \forall b$  (23)

As the solution of the optimization problem in (23) is similar to that in [30], we do not give the details of the solution process.

ii) The joint precoder and receiving equalizer design based on the sum-rate maximization design [20] (denoted as the max-rate design):

$$\begin{aligned} \max_{\mathbf{V}_{k,b},\mathbf{U}_{k,b,\forall k,\forall b}} \sum_{k=1}^{K} \log \left(1 + \gamma_{k,b}\right) \\ \text{s.t.} \quad \gamma_{k,b} \geq \bar{\gamma}_{k,b}, \forall k \\ \|\mathbf{v}_{n,b}\|_{1} \leq \min \left\{p_{n,b} - p_{\min}, \ p_{\max} - p_{n,b}\right\}, \ \forall n, \ \forall b \end{aligned} \tag{24}$$

Since the solution of the optimization problem in (24) is similar to that in [20], we do not give the details of the solution process.

From the above two optimization problem formulations of the MMSE and max-rate designs, we can observe that these two designs still fail to consider both ICI and IUI mitigations simultaneously in multi-user multi-cell VLC systems, resulting in the transmission rate loss according to the rate loss analysis in Section IV-A. Hence, this motivates us to propose the joint precoder and equalizer design based on IA in multi-user multi-cell MIMO VLC systems.

## D. Computational Complexity Analysis

Here, we analyze the computational complexity of the proposed design and compare it with the MMSE and maxrate designs. For our proposed design, in order to update the receiving equalizer  $\mathbf{u}_{k,b}$  for the user (k,b), it requires the following computational operations: (i) computing  $\sum_{b'=1}^{B} \sum_{m=1}^{K} \mathbf{H}_{k,b}^{b'} \mathbf{v}_{m,b'} \mathbf{v}_{m,b'}^{\mathrm{T}} \mathbf{H}_{k,b}^{b'\mathrm{T}}$  in  $O(2BKN_tN_t + 1)$  $BKN_t^2$ ), (ii) computing the inversion in  $O(N_r^3)$ , and (iii) the matrix multiplications of commuting  $\mathbf{H}_{k}^{b'}\mathbf{v}_{m,b'}$  in  $O(N_tN_r)$ . Then, the total computational complexity of updating the receiving equalizers  $\mathbf{u}_{k,b}$ ,  $k=1,\ldots,K$ ,  $b=1,\ldots,B$  for all users in all cells is  $O(BK(2BKN_tN_r + BKN_t^2 + N_tN_r + N_r^3))$ . In order to get the precoder  $\mathbf{v}_{k,b}$ , we directly solve the transformed optimization problem (14) using the CVX software package, and the complexity for the precoder calculation in the problem (14) is  $O(B(N_t + N_r K)^{9/2} \log(1/\zeta))$  [40], where  $\zeta$  is the accuracy target. Then, the overall complexity of the proposed design is  $O(L(BK(BKN_tN_r + BKN_t^2 + N_tN_r +$  $N_r^3 + B(N_t + N_r K)^{9/2} \cdot \log(1/\zeta))$ , where L denotes the number of the iterations until the convergence of the proposed design. When applying the MMSE design, the total complexity of this design is  $O(L(BK(BKN_tN_r + BKN_t^2 + N_tN_r +$  $N_r^3 + B(N_t + N_r K)^{9/2} \log(1/\zeta)$ ). Through the above complexity analysis of the two existing designs, our proposed design has the similar complexity as the MMSE design. It is necessary to note that the proposed design and the MMSE design have a higher computational complexity than that of the max-rate design in multi-user multi-cell MIMO VLC systems, but they can provide a better performance than the max-rate design, and we will give the performance analysis in the next section.

## V. NUMERICAL RESULTS AND DISCUSSIONS

In this section, we evaluate the performance of our proposed joint precoder and equalizer design and compare it with the MMSE design and the max-rate design. In order to make the fair performance comparison, the channel estimation error is considered in both the MMSE and max-rate designs.

The system parameters used in this paper are listed in Table I. The receiving plane is 2.15 m below the room ceiling. For the channel estimation error, we use the normalized error standard deviation:  $\sigma = \delta_e/(||vec(\tilde{\mathbf{H}}_{k,b}^{b'})||_1/N_tN_r)$  [16]. The spacing between two adjacent LED lamps in the same cell and the spacing between two PDs of each user are denoted by  $L_t$  and  $L_r$ , respectively. The four LED lamps in each cell are installed at the center of ceiling. Without loss of generality, the optical power  $p_{n,b}$  of each LED lamp is set to be identical as  $p_{n,b} = p$ ,  $\forall n$ ,  $\forall b$ , and the limited dynamic range of the optical

#### TABLE I SIMULATION PARAMETERS

Parameters	Values		Parameters	Values
Room size (length × width × height)	8 m × 8 m		PD concentrator	1.5
^ width ^ neight )	× 3 m		refractive index	
Number of cells	4		PD area	$0.5 \text{ cm}^2$
Number of LED	2.		Gain of optical	1.0
lamps per cell	2		filter	1.0
Number of users	2		PD responsivity	0.5 A/W
per cell	_			
Number of PDs	2	1	PD full-angle	120°
per user	2		FOV	
LED half-angle	600	1	Crystana handryidth	a 20 MHz
FOV	60°		System bandwidth	
LED Lambertian	1			
emission order	1			

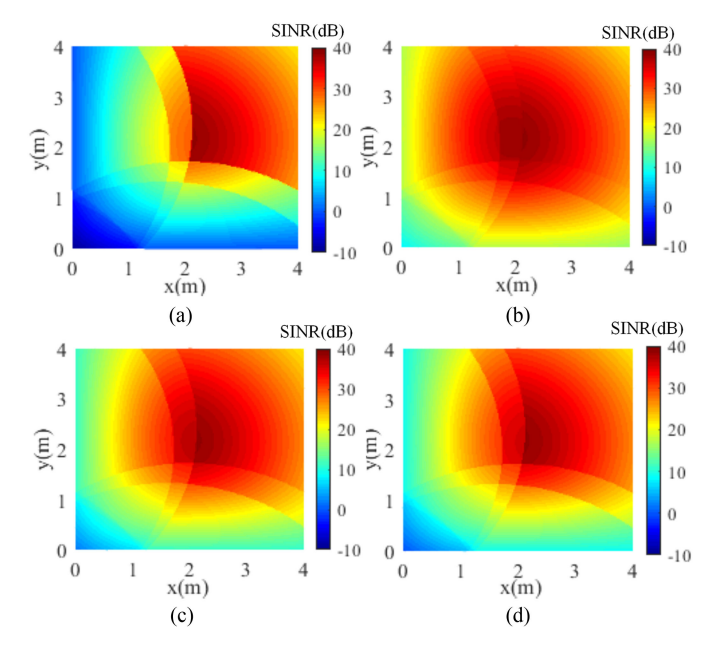


Fig. 2. The SINR distribution. (a) Without any design. (b) With our proposed design. (c) With the MMSE design. (d) With the max-rate design.

power p per LED lamp can be varied from 4 to 22 W (note:  $p_{\min} = 4 \text{ W}$ ,  $p_{\max} = 22 \text{ W}$ ) [41].

## A. Received SINR Distribution

Fig. 2 shows the SINR distributions of one cell (i.e. a quarter of the room) for different designs, where the spacing of LED lamps is  $L_t=0.7\,\mathrm{m}$  and the optical power per LED lamp is 12 W. From Fig. 2, we can observe that the SINR values on the boundaries of adjacent cells are low, especially for the original SINR distribution without any design in Fig. 2(a). However, our proposed joint precoder and equalizer design based on IA significantly outperforms other designs in terms of the average SINR performance on the boundaries of adjacent cells, because our proposed design aims to choose optimal precoders and receiving equalizers based on the IA technique, which can effectively minimize the ICI. Therefore, our proposed design based on IA

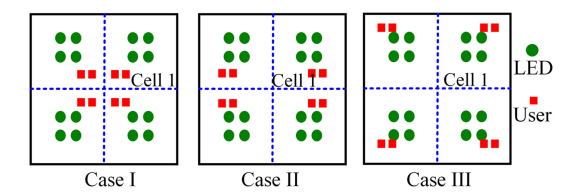


Fig. 3. Three cases of users' locations for the four-cell VLC system.

TABLE II LOCATIONS OF THE IN THE CELL 1 (UNIT: M)

	PDs of User 1	PDs of User 2
Case I	[0.6, 1.0, 0.85] [0.7, 1.0, 0.85]	[1.0, 1.0, 0.85] [1.1, 1.0, 0.85]
Case II	[2.8, 1.0, 0.85]	[3.2, 1.0, 0.85]
G III	[2.9, 1.0, 0.85] [2.8, 3.0, 0.85]	[3.3, 1.0, 0.85]
Case III	[2.9, 3.0, 0.85]	[3.3, 3.0, 0.85]

has the advantage of the ICI suppression in multi-cell VLC systems.

### B. Sum Rate and BER Performance

In this subsection, we evaluate the performance with the three cases of the users locations. Firstly, we give the following three cases of users' locations when the spacing of LED lamps and PDs are  $L_t=0.7\,\mathrm{m}$  and  $L_r=0.07\,\mathrm{m}$ , receptively. The three cases of users locations are shown in Fig. 3. Here, we only give parameters with one quadrant (i.e. Cell 1) of the indoor room in Table II, due to the geometric symmetry of the locations of four cells in the room. Case I: users locate in the totally overlapped area, where they suffer ICI from other three adjacent cells. Case II: users locate in the partially overlapped area, where they suffer ICI only from one adjacent cell. Case III: users locate in the non-overlapped area, where they do not suffer ICI from adjacent cells. All users in the above three cases receive IUI in its own cell.

Figs. 4 and 5 show the throughput and BER performance of the three designs with the different optical power levels and three cases of users locations, when the channel estimation error is  $\sigma=0.025$ . We can see that all the three designs enhance the system performance as the optical power increases when p is less than  $p_{\rm ave}=(p_{\rm min}+p_{\rm max})/2=16$  W, but the performance degrades when p exceeds  $p_{\rm ave}$ . This is because the constraint in (14d) determines the available set of precoding matrix. The feasible range of precoding matrix becomes large as p increases when  $p \leq p_{\rm ave}$ , hence a better solution can be obtained in the system with this broader range of precoding matrix. In contrast, the feasible range of the precoding matrix becomes limited with the increase of p when  $p \geq p_{\rm ave}$ , which degrades the system performance under this situation.

From Figs. 4 and 5, we can observe that the performance of the Case III is better than that of the Cases I and II. This is

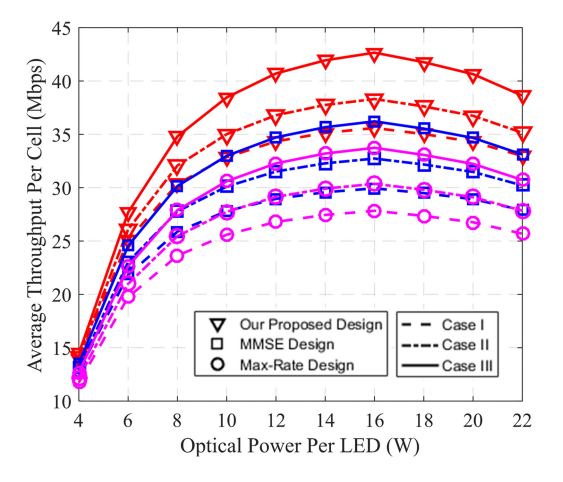


Fig. 4. Average throughput per cell vs. optical power per LED lamp.

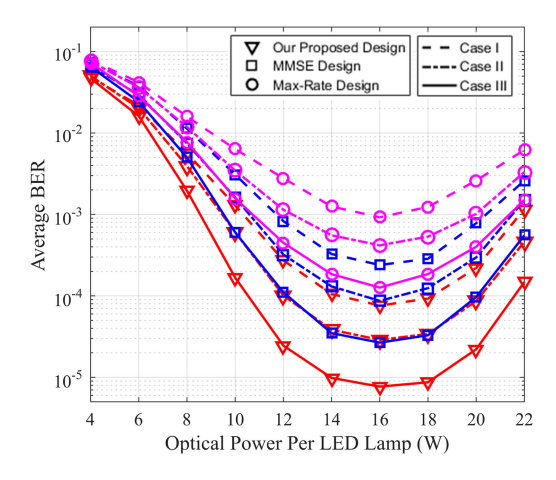


Fig. 5. Average BER performance vs. optical power per LED lamp.

because that the users in last two cases suffer ICI from adjacent cells, which degrades the system performance, especially the users in Case I suffer serious ICI due to their locations in the totally overlapped area.

From Figs. 4 and 5, our proposed design achieves much higher throughput and better BER performance than other two designs. Especially, the advantage becomes more significant in the high optical power region (from 8 to 22 W). This is because the interference is one of the key factors on the data rate loss as the background noise is no longer dominant. Our proposed joint precoder and equalizer design based on IA mitigates both IUI and ICI effectively, and hence the performance is improved compared with other two designs. As shown in Fig. 4, when the optical power is 12 W per LED lamp, our proposed design achieves a throughput improvement of up to 18.2% and 28.7% compared with the MMSE design and the max-rate design under Case I, respectively. As shown in Fig. 5, our proposed design can save about 1.4 and 4.3 W transmit optical power per LED lamp as compared with the MMSE design and the max-rate design at a target BER of 10<sup>-3</sup> under Case I, respectively.

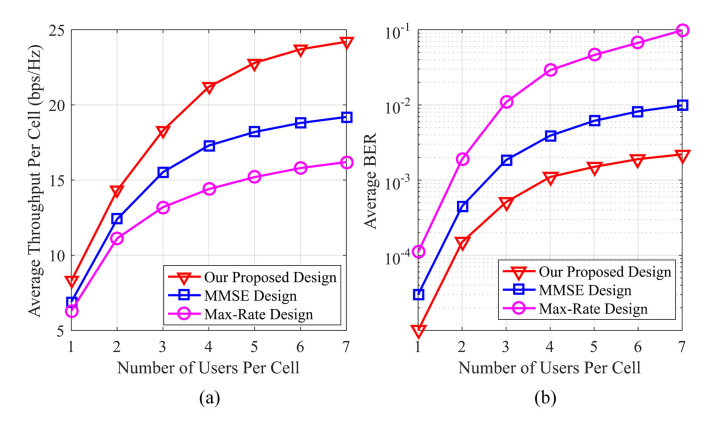


Fig. 6. (a) Average throughput per cell. (b) Average BER vs. different numbers of users per cell.

## C. Impact of Different Numbers of Users Per cell

Figs. 6(a) and (b) show the average throughput per cell and average BER performance under different numbers of users per cell when the optical power per LED is p = 12 W and the channel estimation error is  $\sigma = 0.025$ . (Note: We run the simulation 500 times with random user locations and obtain the average statistics). We can observe that both the average throughput per cell and the average BER increase with the increased number of users per cell. When there are more users within a cell, the interuser interference becomes higher, which has a negative effect on the throughput improvement and the BER performance. That is why the throughput improvement is not obviously when the number of users is large in VLC systems. However, compared with the other designs, the proposed design based on IA has the better performance by effectively suppressing both the IUI and ICI. Moreover, the gap of the performances obtained by the proposed design and the other two designs becomes larger with the increased number of users, which indicates that the proposed design is more suitable for VLC systems with a large number of users.

## D. Impact of Channel Uncertainty and LED/PD Spacing

In Figs. 7(a) and (b), we show the throughput and BER performance for all the three designs under different levels of channel estimation error (we take the Case I as an example), when the optical power per LED is p = 12 W, and the spacing of LED lamps and spacing of PDs are  $L_t=0.7~\mathrm{m}$  and  $L_r=0.07~\mathrm{m}$ , respectively. It can be observed that the performance of all three approaches degrades as the increase of channel estimation error value. This is because under a relatively high channel estimation error value, the optimal design of precoders and receiving equalizers is unable to cancel IUI and ICI perfectly, and hence the degradation of the system performance at the high channel estimation error value becomes obviously. However, among the three designs, the max-rate design is most sensitive to the channel estimation error, while our proposed design based on IA achieves the better performance than other two designs over all the channel estimation error values.

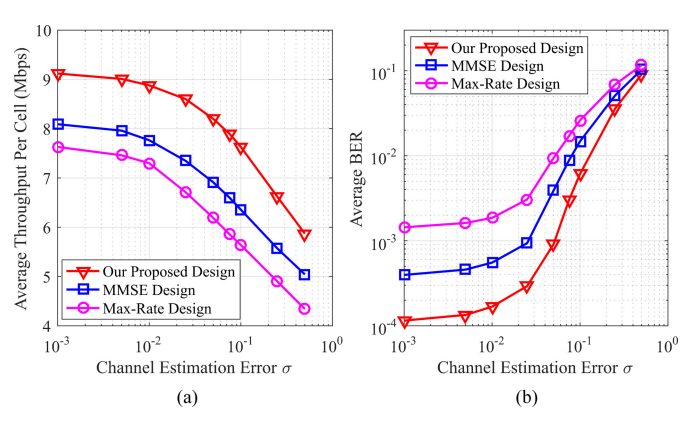


Fig. 7. (a) Average throughput per cell. (b) Average BER against the channel estimation error.

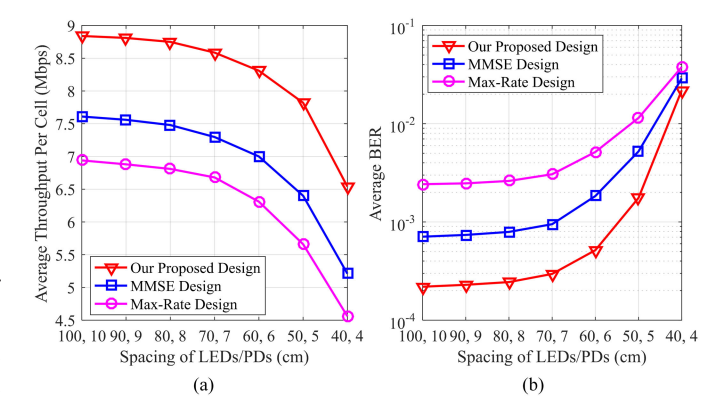


Fig. 8. (a) Average throughput per cell. (b) Average BER vs. the spacing of LEDs/PDs.

Figs. 8(a) and (b) depict the throughput and BER performance for all the three designs with different LED/PD spacing  $(L_t, L_r)$  in cm (we take the Case I as an example), when the optical power per LED lamp is p=12 W and the channel estimation error is  $\sigma=0.025$ . We can see that a smaller LED/PD spacing results in a considerable throughput reduction. This is because the smaller LED/PD spacing leads to a higher channel correlation in the MIMO VLC system, resulting in the noise enhancement at the receivers. However, our proposed design still achieves the best throughput and BER performance among the three designs.

In short, our proposed design achieves the better throughput and BER performance than the other two designs under the different channel estimation error and small LED/PD spacing in multi-user multi-cell MIMO VLC systems.

## E. Convergence of the Three Designs

Fig. 9 presents the performance convergence of the achievable throughput per cell for the three designs when the transmit optical power is 12 W per LED lamp, the channel estimation error is  $\sigma=0.025$  as well as the spacing of LEDs/PDs are  $L_t=0.7$  m and  $L_r=0.07$  m. We can see that the proposed design has almost the same convergence rate as the other two designs, and the throughput converges after about 22 iterations. Moreover,

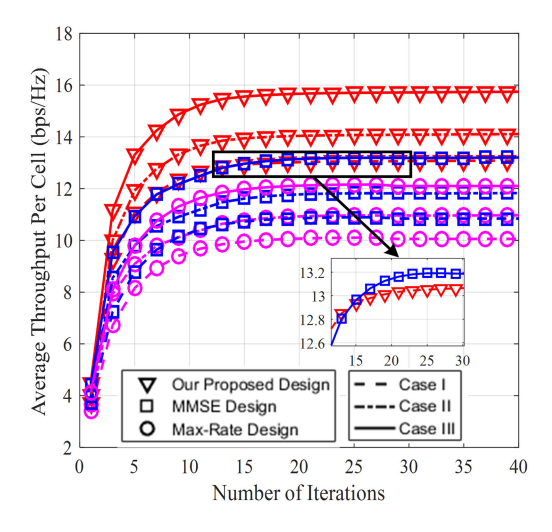


Fig. 9. Convergence for the three designs.

the proposed design achieves the higher throughput than other two designs.

#### VI. CONCLUSION

In this paper, we have proposed a novel joint precoder and receiving equalizer design based on IA for multi-user multi-cell MIMO VLC systems under imperfect CSI, in order to effectively mitigate both IUI and ICI. Specifically, we formulate the joint optimization problem by minimizing the system MSE under the unique optical power constraints in VLC. Furthermore, we take into account the channel estimation error in our formulated optimization problem when designing the optimal precoders and receiving equalizers in multi-user multi-cell MIMO VLC systems. Numerical results show that the proposed design achieves a better system capacity and BER performance as compared with the MMSE and max-rate designs. When the optical power is 12 W per LED lamp, our proposed scheme achieves a throughput improvement of up to 18.2% and 28.7% as compared with the MMSE and max-rate designs, respectively. In addition, the proposed design saves about 1.4 and 4.3 W optical power per LED lamp as compared with the MMSE and max-rate designs, respectively, at a targeted BER of 10<sup>-3</sup>. In our future work, we will apply this design in integrated visible light communication and positioning (VLCP) systems [42].

## REFERENCES

- M. Ayyash et al., "Coexistence of WiFi and LiFi toward 5G: Concepts, opportunities, and challenges," *IEEE Commun. Mag.*, vol. 54, no. 2, pp. 64– 71, Feb. 2016.
- [2] C. Chen, W.-D. Zhong, and D. H. Wu, "On the coverage of multiple-input multiple-output visible light communications [invited]," *J. Opt. Commun. Netw.*, vol. 9, no. 9, pp. 31–41, Aug. 2017.
- [3] T. Q. Wang, R. J. Green, and J. Armstrong, "MIMO optical wireless communications using ACO-OFDM and a prism-array receiver," *IEEE J. Sel. Areas Commun.*, vol. 33, no. 9, pp. 1959–1971, Sep. 2015.
- [4] L. M. Hao et al., "High-speed visible light communications using multiple-resonant equalization," *IEEE Photon. Technol. Lett.*, vol. 20, no. 14, pp. 1243–1245, Aug. 2008.
- [5] C. Chen, W.-D. Zhong, H. L. Yang, and P. F. Du, "On the performance of MIMO-NOMA-based visible light communication systems," *IEEE Pho*ton. Technol. Lett., vol. 30, no. 4, pp. 307–310, Feb. 2018.

- [6] H. Yang, C. Chen, and W. D. Zhong, "Cognitive multi-cell visible light communication with hybrid underlay/overlay resource allocation," *IEEE Photon. Technol. Lett.*, vol. 30, no. 12, pp. 1135–1138, Jun., 2018.
- [7] A. Yesilkaya, E. Basar, F. Miramirkhani, E. Panayirci, M. Uysal, and H. Haas, "Optical MIMO-OFDM with generalized LED index modulation," *IEEE Trans. Commun.*, vol. 65, no. 8, pp. 3429–3441, Aug. 2017.
- [8] C. Chen, S. Videv, D. Tsonev, and H. Haas, "Fractional frequency reuse in DCO-OFDM-based optical attocell networks," *J. Lightw. Technol.*, vol. 33, no. 19, pp. 3986–4000, Oct. 2015.
- [9] C. Chen, W.-D. Zhong, H. L. Yang, S. Zhang, and P. F. Du, "Reduction of SINR fluctuation in indoor multi-cell VLC systems using optimized angle diversity receiver," *J. Lightw. Technol.*, vol. 36, no. 17, pp. 3603–3610, Sep. 2018.
- [10] T. V. Pham, H. L. Minh, and A. T. Pham, "Multi-cell VLC: multi-user downlink capacity with coordinated precoding," in *Proc. IEEE Int. Conf. Commun.*, Paris, May 2017, pp. 469–474.
- [11] Y. J. Zhu, W. Y. Wang, and G. Xin, "Faster-than-Nyquist signal design for multiuser multicell indoor visible light communications," *IEEE Photon.* J., vol. 8, no. 1, Feb. 2016, Art. no. 7902012.
- [12] K. X. Zhou, C. Gong, Q. Gao, and Z. Y. Xu, "Inter-cell interference coordination for multi-color visible light communication networks," in *Proc. IEEE GlobalSIP*, Dec. 2016, pp. 1–6.
- [13] S. Y. Jung, D.-H. Kwon, S.-H. Yang, and S.-K. Han, "Inter-cell interference mitigation in multi-cellular visible light communications," *Opt. Express*, vol. 24, no. 8, pp. 8512–8526, Apr. 2016.
- [14] H. N. Ryoo, D. H. Kwon, S. H. Yang, and S. K. Han, "Differential optical detection in VLC for inter-cell interference reduced flexible cell planning," *IEEE Photon. Technol. Lett.*, vol. 28, no. 23, pp. 2728–2731, Dec. 2016.
- [15] H. Ma, L. Lampe, and S. Hranilovic, "Integration of indoor visible light and power line communication systems," in *Proc. 17th IEEE ISPLC*, *Johannesburg*, Africa, Mar. 2013, pp. 291296.
- [16] H. Ma, L. Lampe, and S. Hranilovic, "Coordinated broadcasting for multiuser indoor visible light communication systems," *IEEE Trans. Commun.*, vol. 63, no. 9, pp. 3313–3324, Sep. 2015.
- [17] T. V. Pham and A. T. Pham, "Cooperation strategies and optimal precoding design for multi-user multi-cell VLC networks," *Proc. IEEE Global Commun. Conf.*, Singapore, Dec. 2017, pp. 1–6.
- [18] J. Lian and M. Brandt-Pearce, "Multiuser MIMO indoor visible light communication system using spatial multiplexing," *J. Lightw. Technol.*, vol. 35, no. 23, pp. 5024–5033, Dec. 2017.
- [19] B. Li, J. Wang, R. Zhang, H. Shen, C. Zhao, and L. Hanzo, "Multiuser MISO transceiver design for indoor downlink visible light communication under per-LED optical power constraints," *IEEE Photon. J.*, vol. 7, no. 4, Aug. 2015, Art. no. 7201415.
- [20] H. Shen, Y. Deng, W. Xu, and C. Zhao, "Rate maximization for downlink multiuser visible light communications," *IEEE Access*, vol. 4, pp. 6567–6573, 2016.
- [21] Q. Wang, Z. Wang, and L. Dai, "Multiuser MIMO-OFDM for visible light communications," *IEEE Photon. J.*, vol. 7, no. 6, pp. 1–11, Dec. 2015.
- [22] H. Marshoud, P. C. Sofotasios, S. Muhaidat, S. S. Bayan, and K. K. George, "Optical adaptive precoding for visible light communications," *IEEE Access*, vol. 6, pp. 22121–22130, Mar. 2018, [Online]. Available: https://arxiv.org/abs/1612.04937
- [23] N. Huang, X. Wang, and M. Chen, "Transceiver design for MIMO VLC systems with integer-forcing receivers," *IEEE J. Sel. Areas Commun.*, vol. 36, no. 1, pp. 66–77, Jan. 2018.
- [24] V. R. Cadambe and S. A. Jafar, "Interference alignment and degrees of freedom of the K-user interference channel," *IEEE Trans. Inf. Theory*, vol. 54, no. 8, pp. 3425–3441, Aug. 2008.
- [25] A. Motahari, S. Oveis-Gharan, M.-A. Maddah-Ali, and A. Khandani, "Real interference alignment: exploiting the potential of single antenna systems," *IEEE Trans. Inf. Theory*, vol. 60, no. 8, pp. 4799–4810, Aug. 2014.
- [26] S. M. Razavi and T. Ratnarajah, "Adaptive LS- and MMSE-based beamformer design for multiuser MIMO interference channels," *IEEE Trans. Veh. Technol.*, vol. 65, no. 1, pp. 132–144, Jan. 2016.
- [27] X. Xie, H. Yang, and A. V. Vasilakos, "Robust transceiver design based on interference alignment for multi-user multi-cell MIMO networks with channel uncertainty," *IEEE Access*, vol. 5, pp. 5121–5134, May 2017.
- [28] X. Zhang, Q. Gao, and Z. Xu, "Optical interference alignment for an indoor visible light communication X-channel," in *Proc. IEEE GlobalSIP*, Orlando, FL, 2015, pp. 1175–117.

- [29] L. Wu, Z. Zhang, J. Dang, and H. Liu, "Blind interference alignment for multiuser MISO indoor visible light communications," *IEEE Commun. Lett.*, vol. 21, no. 5, pp. 1039–1042, Jan. 2017.
- [30] K. Ying, H. Qian, R. J. Baxley, and S. Yao, "Joint optimization of precoder and equalizer in MIMO VLC systems," *IEEE J. Sel. Areas Commun.*, vol. 33, no. 9, pp. 1949–1958, Sep. 2015.
- [31] T. Fath and H. Haas, "Performance comparison of MIMO techniques for optical wireless communications in indoor environments," *IEEE Trans. Commun.*, vol. 61, no. 2, pp. 733–742, Feb. 2013.
- [32] M. Morales-Cspedes, M. C. Paredes-Paredes, A. Garca Armada, and L. Vandendorpe, "Aligning the light without channel state information for visible light communications," *IEEE J. Sel. Areas Commun.*, vol. 36, no. 1, pp. 91–105, Jan. 2018.
- [33] O. B. Usman, J. A. Nossek, C. A. Hofmann, and A. Knopp, "Joint MMSE precoder and equalizer for massive MIMO using 1-bit quantization," in *Proc. IEEE Int. Conf. Commun.*, Paris, May 2017, pp. 1–6.
- [34] R. Mai, D. H. N. Nguyen, and T. Le-Ngoc, "Joint MSE-based hybrid precoder and equalizer design for full-duplex massive MIMO systems," in *Proc. IEEE Int. Conf. Commun.*, Kuala Lumpur, 2016, pp. 1–6.
- [35] H. Elgala, R. Mesleh, and H. Haas, "An LED model for intensity modulated optical communication systems," *IEEE Photon. Technol. Lett.*, vol. 22, no. 11, pp. 835–837, Jun. 2010.
- [36] M. J. Kim, H. H. Lee, and Y. C. Ko, "Robust transceiver design based on joint signal and interference alignment for MIMO interference channels with imperfect channel knowledge," *IEEE Commun. Lett.*, vol. 18, no. 11, pp. 2035–2038, Nov. 2014.
- [37] R. Horn and C. Johnson, *Topics in Matrix Analysis*. New York, NY, USA: Cambridge Univ. Press, 1991.
- [38] CVX Research, Inc., "CVX: Matlab software for disciplined convex programming, version 2.0 (beta)," Jun. 2013.
- [39] N. Jindal, "MIMO broadcast channels with finite-rate feedback," IEEE Trans. Inf. Theory, vol. 52, no. 1, pp. 5045–5060, Nov. 2006.
- [40] Z.-Q. Luo, W.-K. Ma, A.-C. So, Y. Ye, and S. Zhang, "Semidefinite relaxation of quadratic optimization problems," *IEEE Signal Process. Mag.*, vol. 27, no. 3, pp. 20–34, May 2010.
- [41] Y.-J. Lee et al., "Study of GaN-based light-emitting diodes grown on chemical wet-etching-patterned sapphire substrate with v-shaped pits roughening surfaces," J. Lightw. Technol., vol. 26, no. 11, pp. 1455–1463, Jun. 2008.
- [42] H. L. Yang, C. Chen, W.-D. Zhong, A. Alphones, S. Zhang, and P. Du, "Demonstration of a quasi-gapless integrated visible light communication and positioning system," appear in *Proc. IEEE Photon. Technol. Lett.*, 2018.



Chen Chen (S'13) received both the B.S. and M.Eng. degrees from the University of Electronic Science and Technology of China, Chengdu, China, in 2010 and 2013, respectively, and the Ph.D. degree from Nanyang Technological University, Singapore, in 2017. He is currently a Postdoctoral Research Fellow with the School of Electrical and Electronic Engineering, Nanyang Technological University. His research interests include visible light communications, visible light positioning, optical access networks, and digital signal processing. He received the Best Paper

Award at the IEEE Photonics Global Conference in 2015. He was a recipient of the outstanding reviewer certificates from Elsevier Optical Fiber Technology and Digital Signal Processing in 2017 and 2018, respectively. He received the Publons Peer Review Awards in both engineering and physics in 2018. He was also a co-recipient of the IET Optoelectronics Premium Award in 2018.



Wen-de Zhong (SM'03) was a Postdoctoral Fellow with NTT Network Service and System Laboratories, Japan, from 1993 to 1995. He was a Senior Research Fellow with the Department of Electrical and Electronic Engineering, University of Melbourne, Australia, from 1995 to 2000. He joined Nanyang Technological University, Singapore, in 2000, as an Associate Professor and became a Full Professor in 2009, and is currently with the School of Electrical and Electronic Engineering. He has coauthored more than 250 refereed journal and conference papers. His

current research interests include visible light communication/positioning, optical fiber communication systems and networks, optical access networks, and signal processing. He was in the organizing and/or technical program committee for numerous international conferences, including ECOC, ICC, GLOBECOM, OECC, ICICS, and ICOCN. He is currently an Associate Editor of the IEEE ACCESS and also an Editor of *Unmanned Systems*.



Helin Yang (S'15) is currently working toward Ph.D. degree in the School of Electrical and Electronic Engineering, Nanyang Technological University, Singapore. He received the B.S. and M.S. degrees in the School of Telecommunications and Information Engineering from the Chongqing University of Posts and Telecommunications, Chongqing, China, in 2013, and 2016, respectively. He is a Reviewer for the international journals such as IEEE COMMUNICATIONS MAGAZINE, IEEE TRANSACTIONS ON WIRELESS COMMUNICATIONS, IEEE TRANSACTIONS

ON VEHICULAR TECHNOLOGY. His current research interests include wireless communication, visible light communication, and resource management.



Arokiaswami Alphones (M'92–SM'98) received the B.Tech. degree from the Madras Institute of Technology, Chennai, India, in 1982, the M.Tech. degree from the Indian Institute of Technology Kharagpur, Kharagpur, India, in 1984, and the Ph.D. degree in optically controlled millimeter wave circuits from the Kyoto Institute of Technology, Kyoto, Japan, in 1992. During 1997–2001, he was with the Center for Wireless Communications, National University of Singapore, where he was involved in the research on optically controlled passive/active devices. Since

2001, he has been with the School of Electrical and Electronic Engineering, Nanyang Technological University, Singapore. He is also the Program Coordinator for research. He has 30 years of research experience. He has authored or coauthored and presented more than 250 technical papers in peer-reviewed international journals/conferences. His current research interests include electromagnetic analysis on planar RF circuits and integrated optics, microwave photonics, metamaterial-based leaky wave antennas, and wireless power transfer technologies. He was a JSPS Visiting Fellow from 1996 to 1997 at Japan. He was involved in many IEEE flagship conferences held in Singapore and General Chair of APMC 2009, and MWP 2011. He is currently the Chairman of the IEEE Singapore section.